

Data Reduction with NIRA

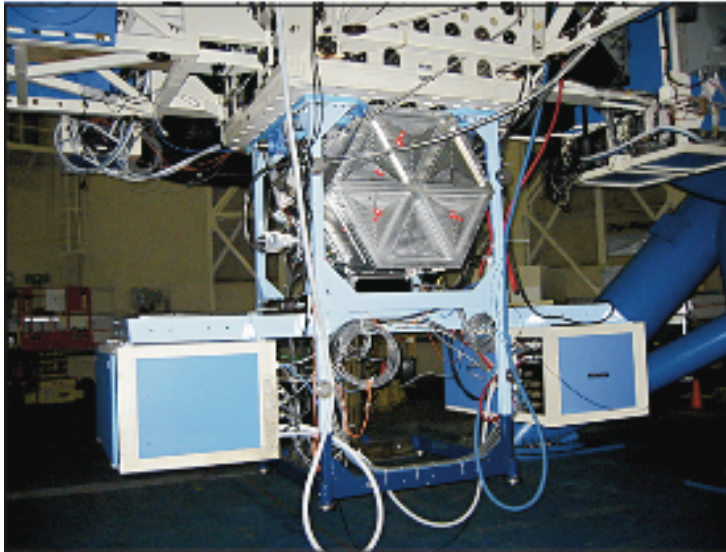
Knut Olsen and Andrew Stephens

Gemini Data Workshop

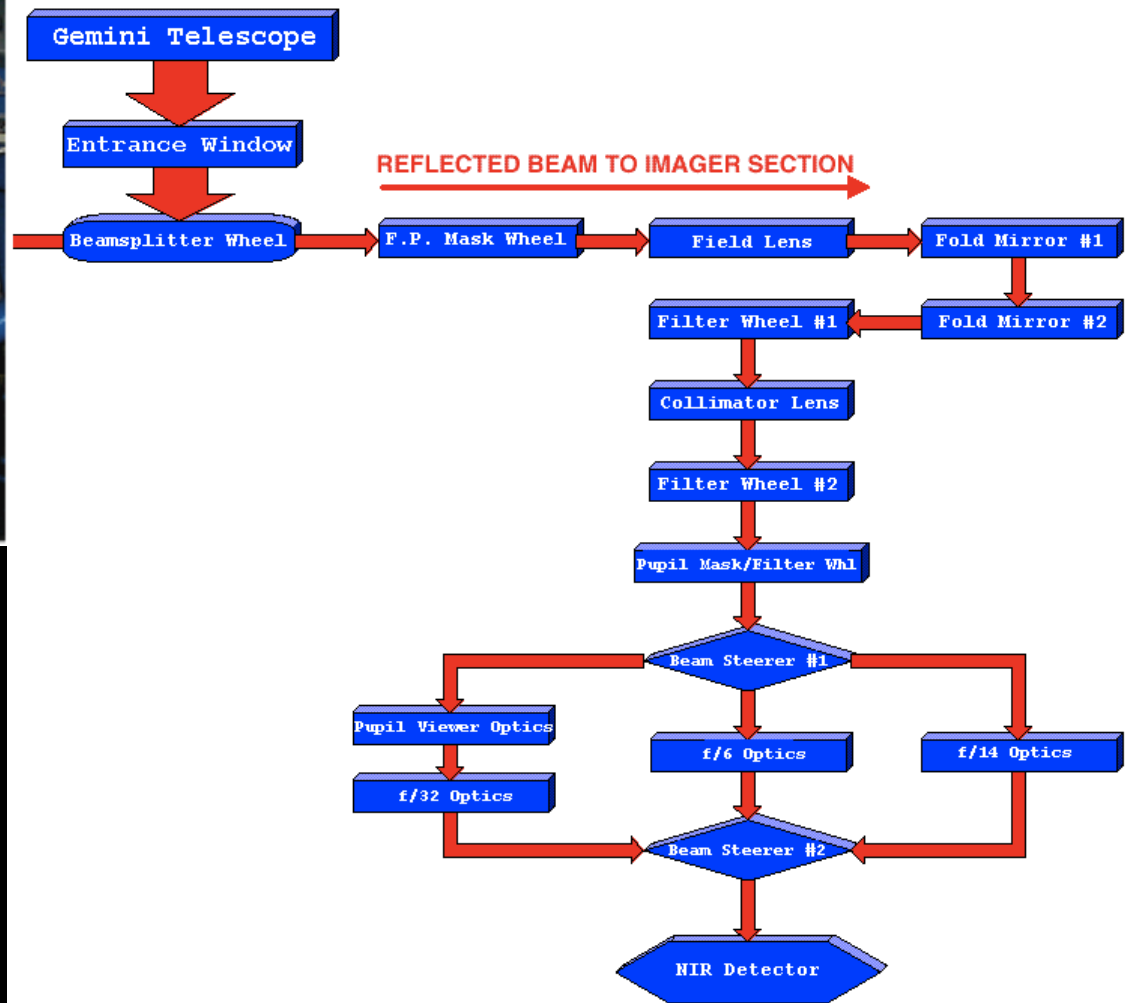
Tucson, AZ

July 21, 2010

Near InfraRed Imager and Spectrometer



- *Built by UH/IfA*
- *Science data since 2002*
- *Primary reference: Hodapp et al. (2003)*



NIRI Instrument Properties

Detector 1024 × 1024 pixel ALADDIN InSb array,
sensitive from 1 to 5 μm .

The Aladdin detector has uniform response and low dark current. Various size centered subarrays may be read out instead of the full 1024×1024 array. The bias voltage may be adjusted to modestly increase the well depth for thermal IR (L and M band) observations. The NIRI array is read out in different modes for different kinds of observations that trade read noise against integration time:

1) at **high background** (e.g., thermal IR), the array is read once at the beginning and once at the end of the exposure and the difference is recorded; $\text{RN}=70e^-$, min exp time is 0.18 sec*

2) at **medium background** (e.g., broad band JHK imaging) the same basic mode is used, but beginning and end reads are digitally averaged 16 times; $\text{RN}=35e^-$, min exp time is 0.55 sec*

3) at **low background** (e.g., 1-2.5 μm narrow band imaging and 1-2.5 μm faint object spectroscopy), the array is read 16 times at the beginning and the end of the exposure, with the above digital averaging also taking place during each read; $\text{RN}=12e^-$, min exp time is 8.8 sec*

**numbers given are for full array*

Imaging Mode

Three Cameras and Pixel Scales:

- f/32 at 0.022 arcsec/pixel over 22×22 arcsec
- f/14 at 0.050 arcsec/pixel over 51×51 arcsec
- f/6 at 0.117 arcsec/pixel over 120×120 arcsec

Filters: J, H, K, K_s , K' , L', M' broad-band filters and a full complement of line and feature narrow-band filters

Spectroscopic Mode

- Moderate resolution long-slit grism spectroscopy
- The available slit widths (optimized for the f/6 camera) are ~ 0.23, 0.46, and 0.69 arcsec (2, 4, and 6 pixels) wide and 50 arcsec long.

- Spectral Resolution over each complete spectroscopic band: J (770/610/460), H (1650/825/520), K (1300/780/550), L (1100/690/460), M (1100/690/460)

Guiding Options – Guide Stars

The peripheral wavefront sensors (PWFS), which are usable in a number of optical bands and cover up to a 7 arcmin patrol field (but are not mechanically part of NIRI), can be employed to provide fast guiding, focus, and low order M1 adjustments. PWFS2 should be used for most programs.

NIRI has a near-IR on-instrument wavefront sensor (OIWFS) to provide fast guiding information in optically obscured regions or to account for flexure between NIRI and the adaptive optics system (see below).

The OIWFS is not currently available.

Adaptive Optics

NIRI can operate in conjunction with Altair, a natural guide star and laser guide star adaptive optics system for the Gemini North telescope built at the Herzberg Institute for Astronomy. Both imaging and spectroscopy are supported at f/32:

- 1-2.5 μm imaging (broad band and narrow band filters) and L' (for point sources)
- 1-2.5 μm low resolution grism spectroscopy. Slit widths at f/32 are 0.09, 0.14, 0.23 arcsec. Spectral resolutions are similar to those for f/6; see the NIRI Web pages for details.
- In natural guide star mode, Altair uses a bright nearby ($R < 15$ within 25 arcsec) star to provide AO correction. See Altair Web pages for details.
- A laser guide star (LGS) is available for use with Altair. Tip-tilt natural guide stars must be available ($R < 18$ within 25 arcsec). See Altair Web pages for details.

Telescope - Gemini North

NIRI is available for use in both queue and classical observing modes.

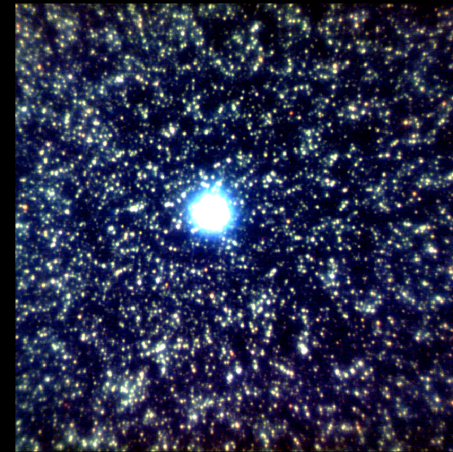
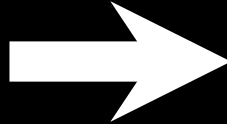
Relevant News

- ✦ 2010 April 29: Beam splitter wheel locked in f/6 position
- ✦ 2010 June 21: Focal Plane Unit became stuck, locked in f/6 imaging position

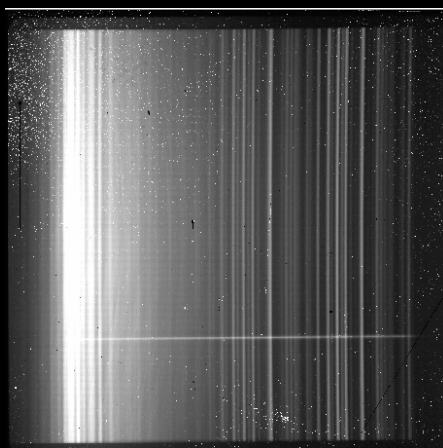
Goals



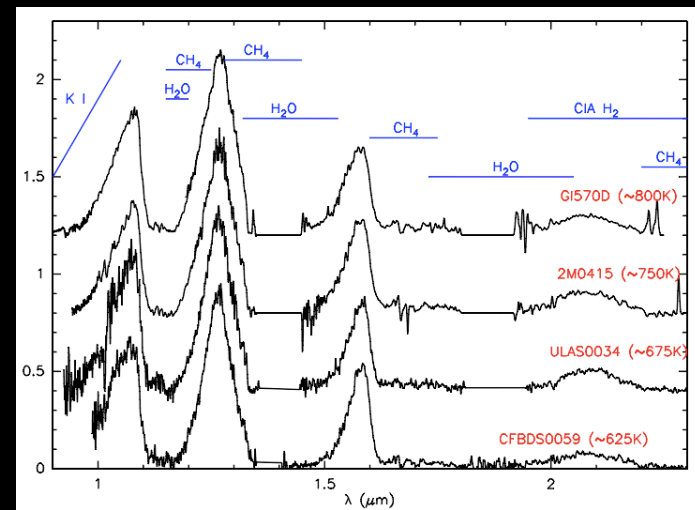
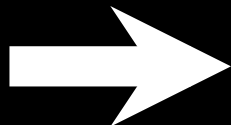
Altair SV dataset



Davidge et al. (2005), Olsen et al. (2006)



GN-2007B-Q-3 (PI Albert)



Delorme et al. (2008)

Preliminaries

- Will use Gemini IRAF package, following NIRI examples
- Additional important NIRI tools: `nirlin.py` and `nirinoise.py` courtesy of Andrew Stephens
- Andy Stephens provided spectroscopic reduction example

The Bulge and Disk of M31

- Nearby:

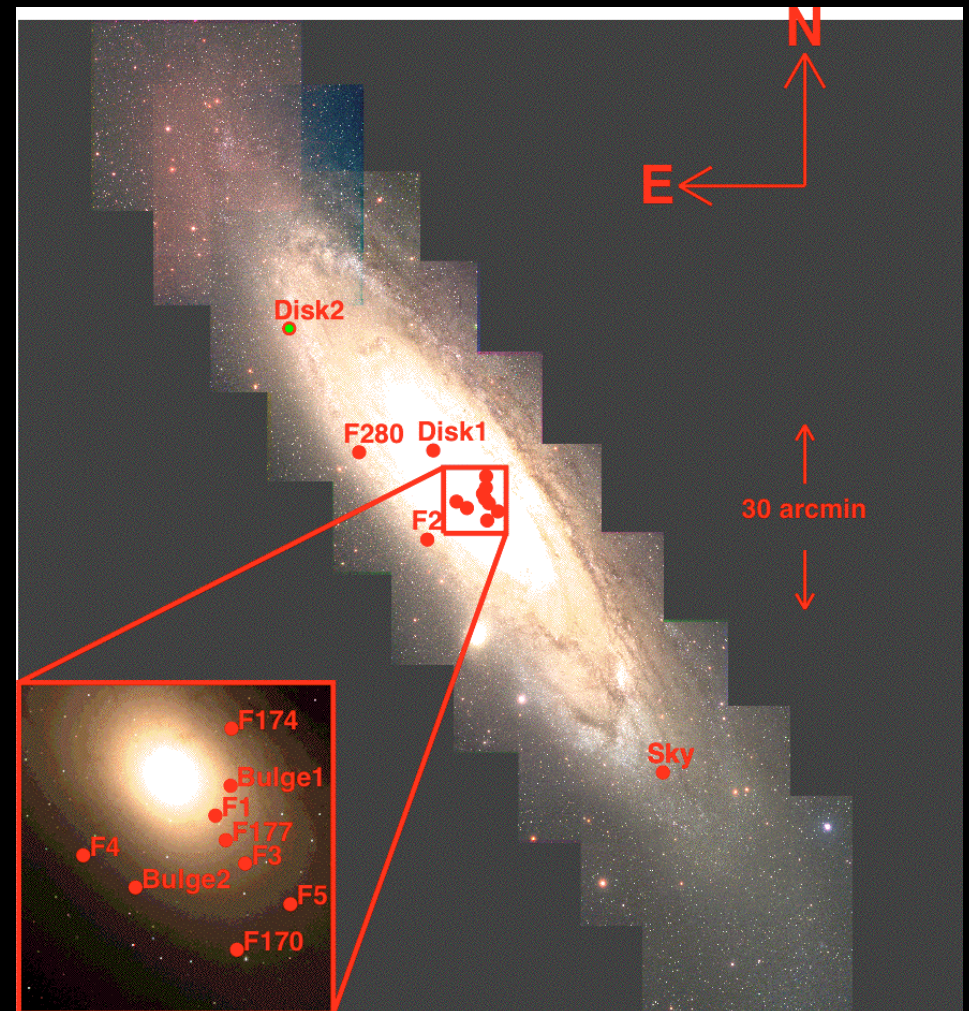
Can study *entire* star formation history from its resolved stars

Complementary to studies of galaxies with $z > 0.5$, which are limited to integrated broadband photometry or IFU spectroscopy

- Extragalactic:

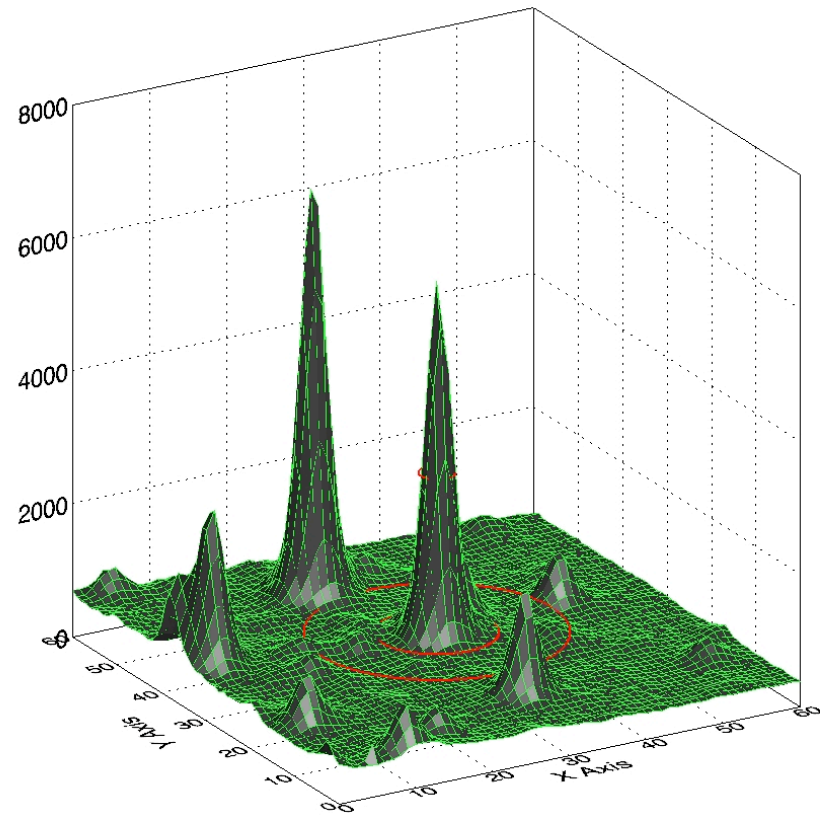
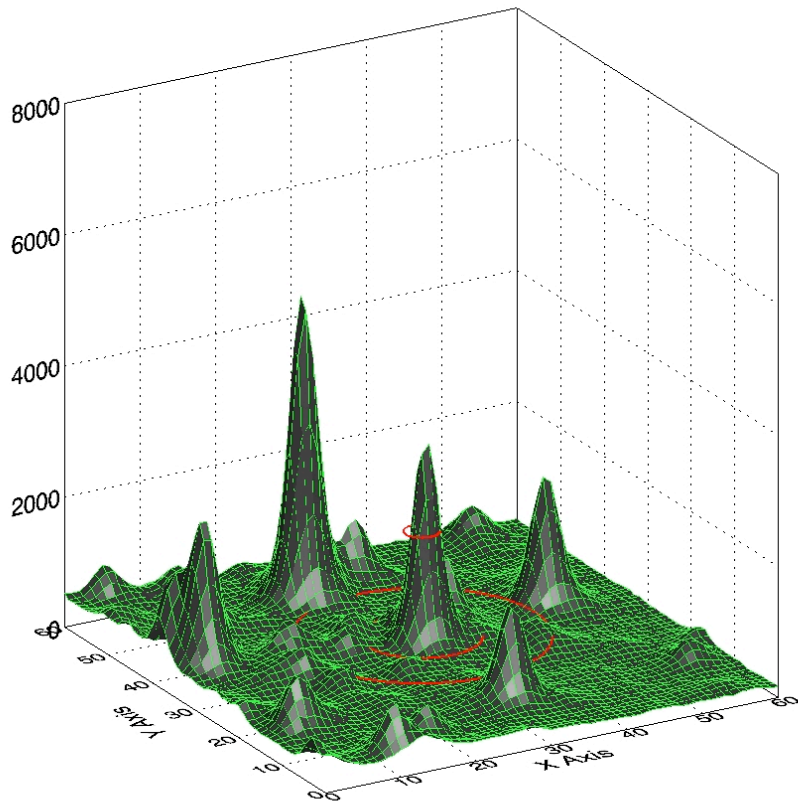
Can easily trace contributions from different galactic components

Milky Way produces important constraints on the stellar populations of galactic components, but from large and heterogeneous datasets



Why Adaptive Optics?

Crowding introduces photometric error through luminosity fluctuations within a *single* resolution element of the telescope due to the unresolved stellar sources in that element.



To calculate the effects of crowding on magnitudes and colors, we need only consider the Poisson statistics of the luminosity functions (e.g. Tonry & Schneider 1988)

For magnitudes:

$$\Sigma_b > 2M - 2.5 \log \left(\frac{4}{\pi} \left(\frac{\sigma_m}{1.086 a_{\text{res}}} \right)^2 \frac{\int_{M_{\text{lo}}}^{M_{\text{hi}}} 10^{-0.4M'} N(M') dM'}{\int_{M_{\text{lo}}}^M 10^{-0.8M'} N(M') dM'} \right) + (m - M)_\circ$$

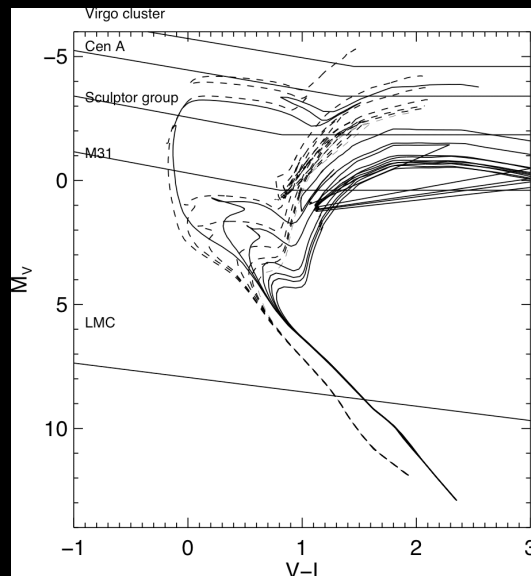
For colors:

$$\sigma_{m_1 - m_2}^2 = \sigma_{m_1}^2 + \sigma_{m_2}^2 - 2\sigma_{m_1 m_2}^2$$

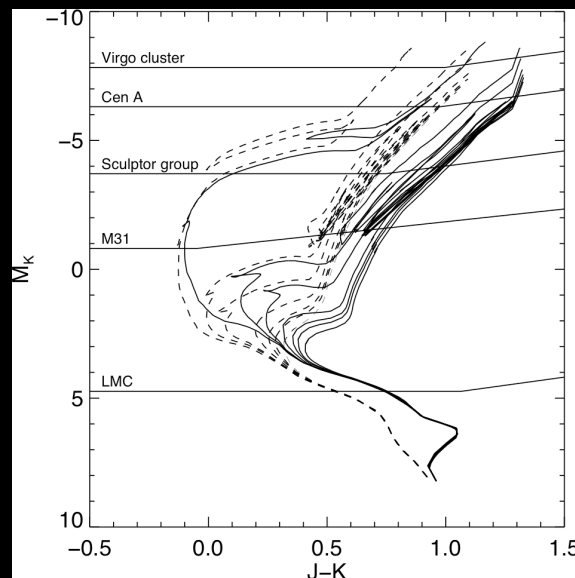
$$\sigma_{m_1 m_2}^2 = \frac{1.086}{\sqrt{L_1 L_2}} \frac{\pi \Sigma_{L_1} \min(a_1^2, a_2^2)}{4 \int_0^\infty \int_0^\infty l_1 N_{12}(l_1, l_2) dl_1 dl_2} \int_0^{L_1} \int_0^{L_2} l_1 l_2 N_{12}(l_1, l_2) dl_1 dl_2$$

Crowding limits for current and future telescopes

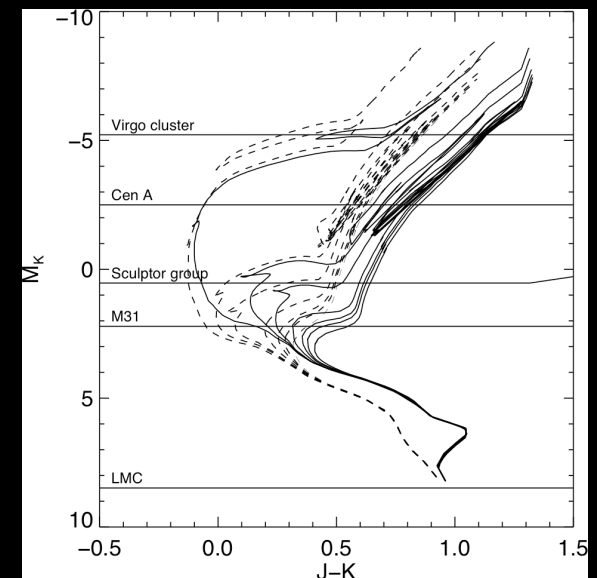
HST (optical)



Gemini North



30-m (near-IR)



Magnitudes at which 10% photometry is possible in regions of surface brightness $\Sigma_V=22$, $\Sigma_K=19$ for galaxies at the indicated distances.

Observations

Gemini N+Altair/NIRI SV
observations, 18-19 Nov 2003
(one night photometric)

Disk 2 field observed 14 Sep
2006: 0.''2 - 0.''3 seeing,
photometric

NIRI/Altair provided near
diffraction-limited imaging in HK
over $22.''5 \times 22.''5$ field

We also include published HST/
NICMOS data from Stephens et
al. (2003)

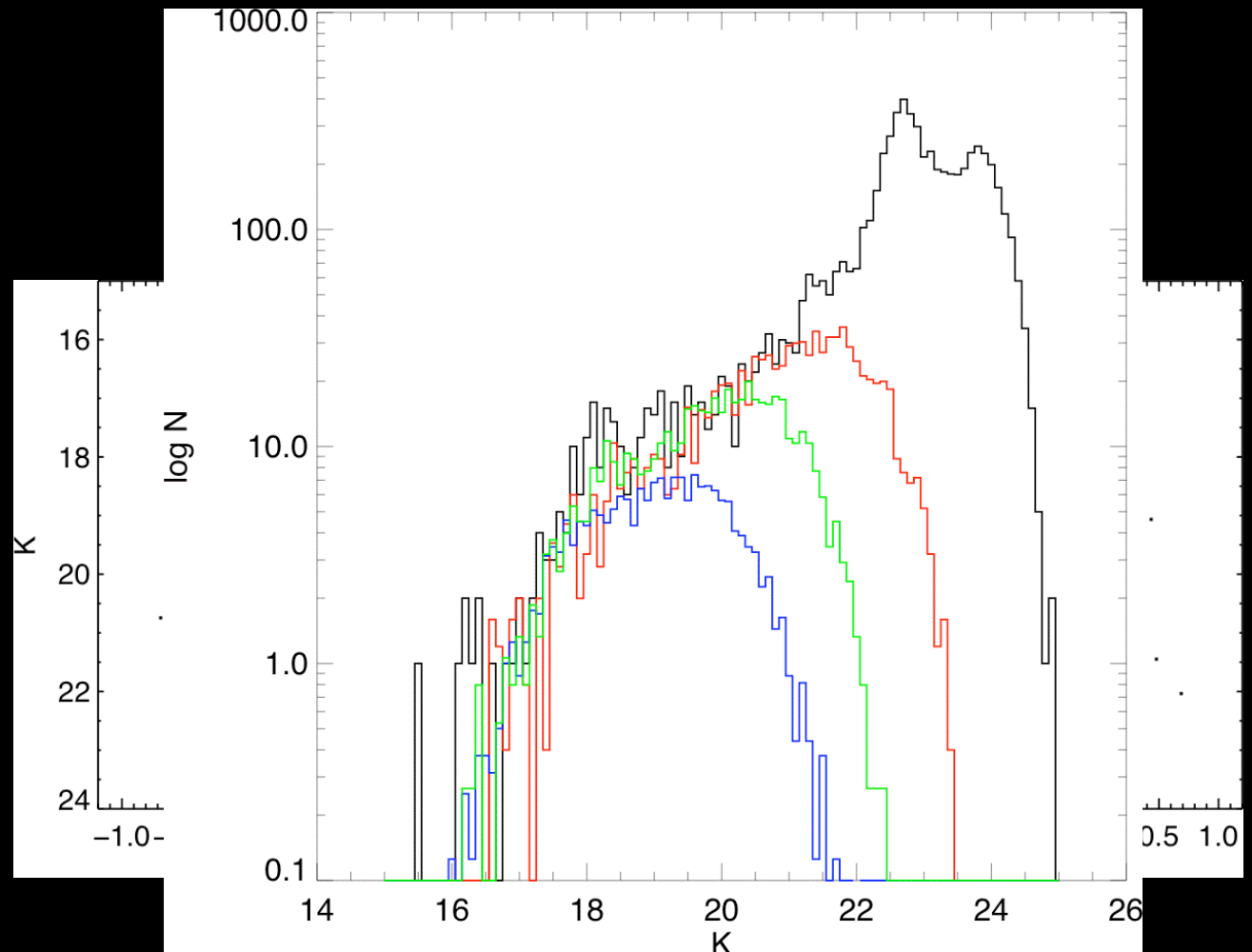


Disk 2: 540s H, 3420s K

0.''059 H (~30% Strehl), 0.''066 K (~40% Strehl)

Analysis

- Usefully measure stars as faint as $M_K = -4$ to -5 (includes TRGB) in bulge and inner disk (published in Davidge et al. (2005) and Olsen et al. (2006))
- Disk 2 field reaches level of horizontal branch



Photometry

- PSF-fitting photometry with DAOPHOT/ALLSTAR

Fits the core of the PSF (0."44 diameter), neglecting the halo

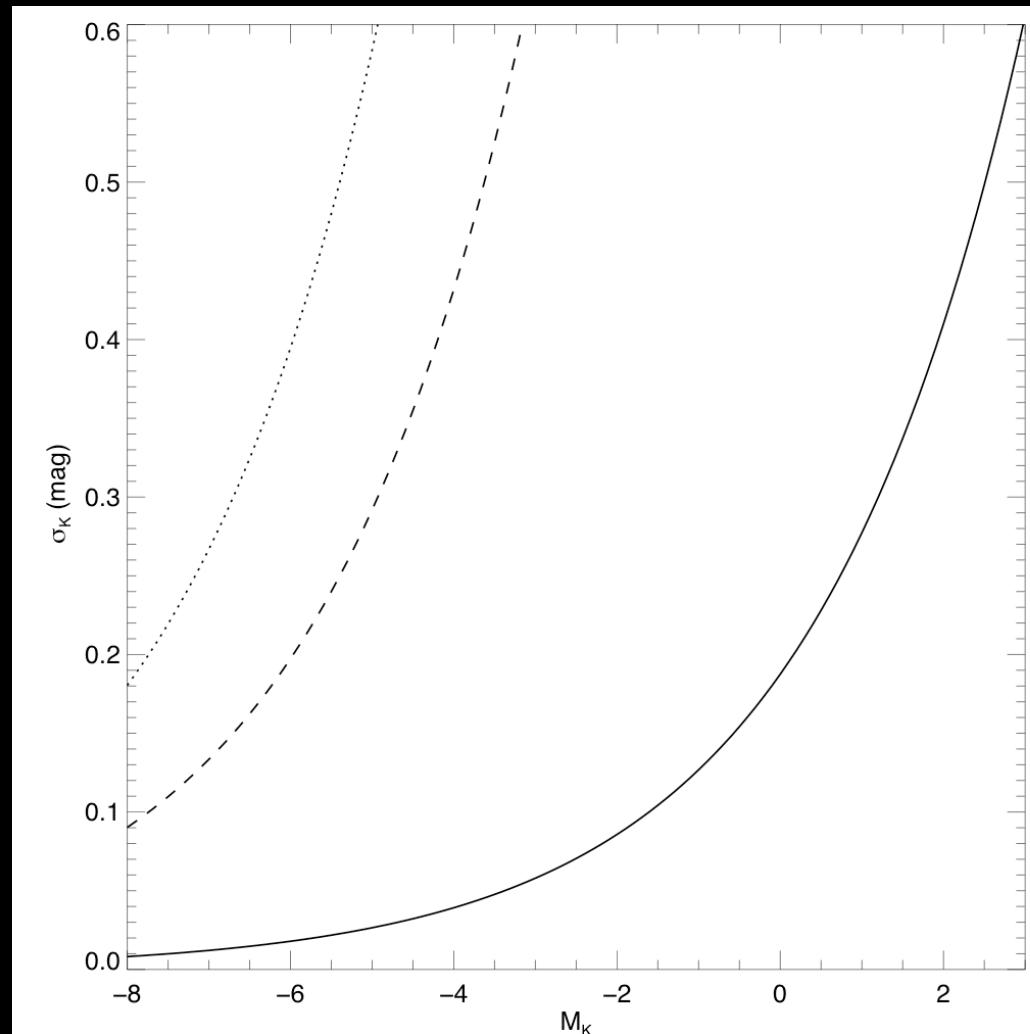
- Corrections applied to account for:

- difference between PSF and aperture magnitudes out to a diameter of 0."66 (30 pixels): ~ 0.3 mags

- difference between 0."66 diameter aperture magnitudes and 4."4 diameter aperture magnitudes: $\sim 0.4 - 0.6$ mags

- spatial variability of the aperture correction

- transformation of magnitudes to standard system



Photometric quality

- PSF-fitting photometry with DAOPHOT/ALLSTAR

Fits the core of the PSF (0.''44 diameter), neglecting the halo

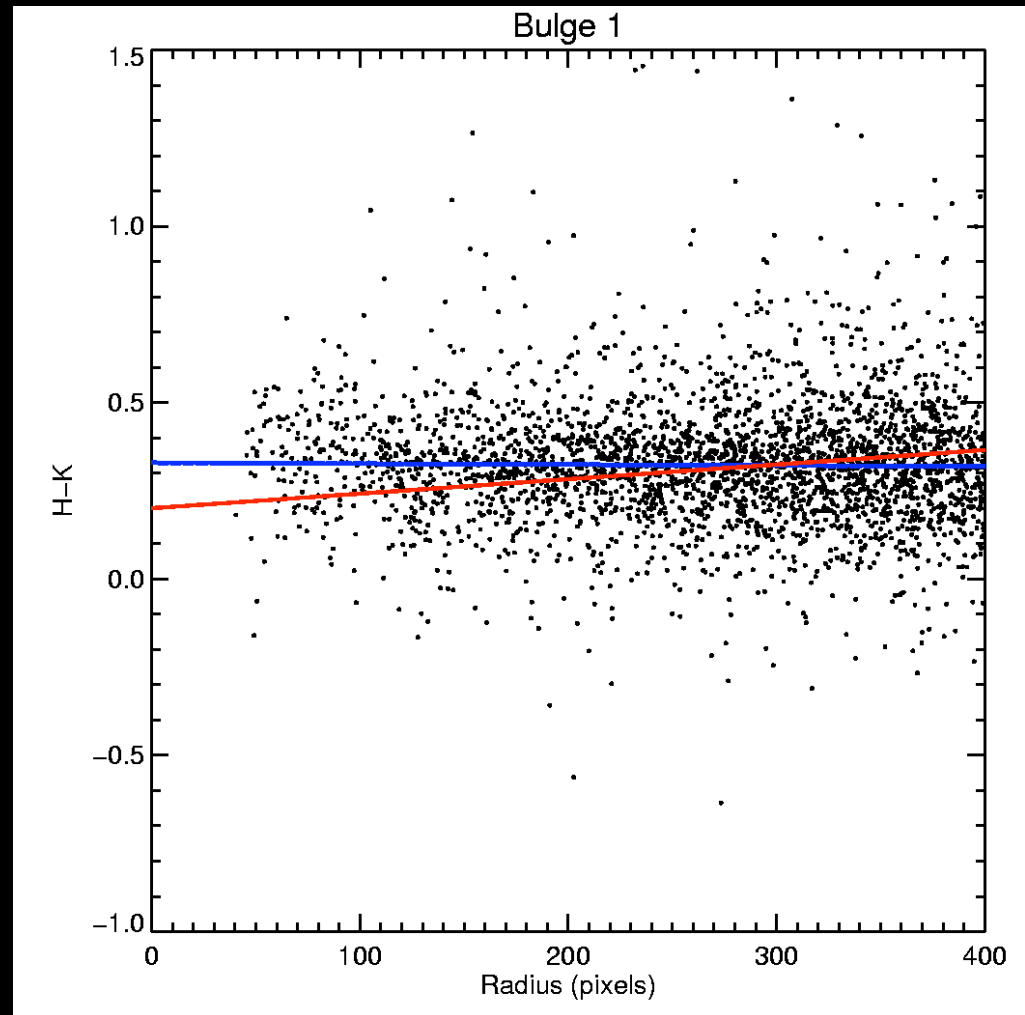
- Corrections applied to account for:

- difference between PSF and aperture magnitudes out to a diameter of 0.''66 (30 pixels):
~0.3 mags

- difference between 0.''66 diameter aperture magnitudes and 4.''4 diameter aperture magnitudes: ~0.4 - 0.6 mags

- spatial variability of the aperture correction

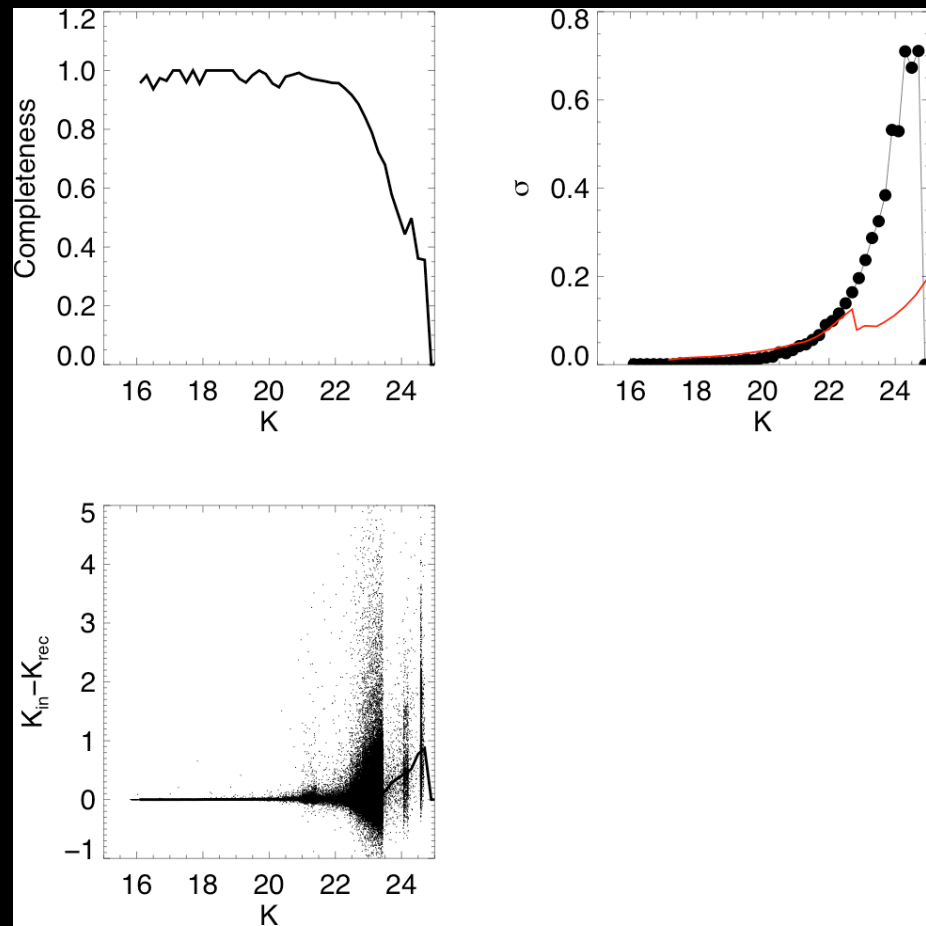
- transformation of magnitudes to standard system



Photometric error analysis

- Completeness and photometric errors calculated from extensive Monte Carlo simulations
- Both simulations and analytical crowding calculation (Olsen, Blum, & Rigaut 2003) indicate that crowding dominates errors for bulge and inner disk; do not go as deep as expected in Disk 2 field
- Restrict analysis to magnitudes with >50% completeness

Disk 2 field



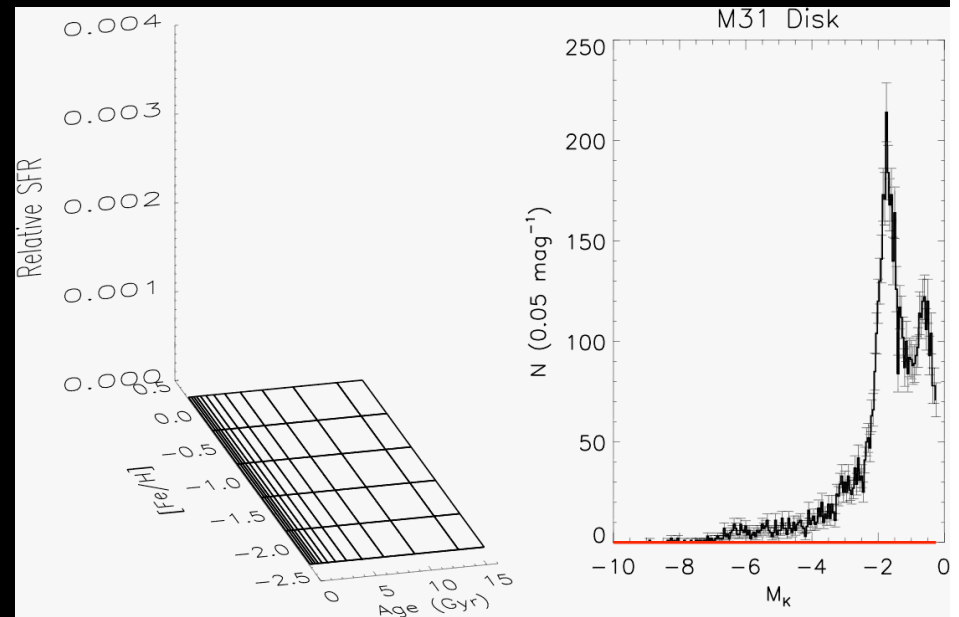
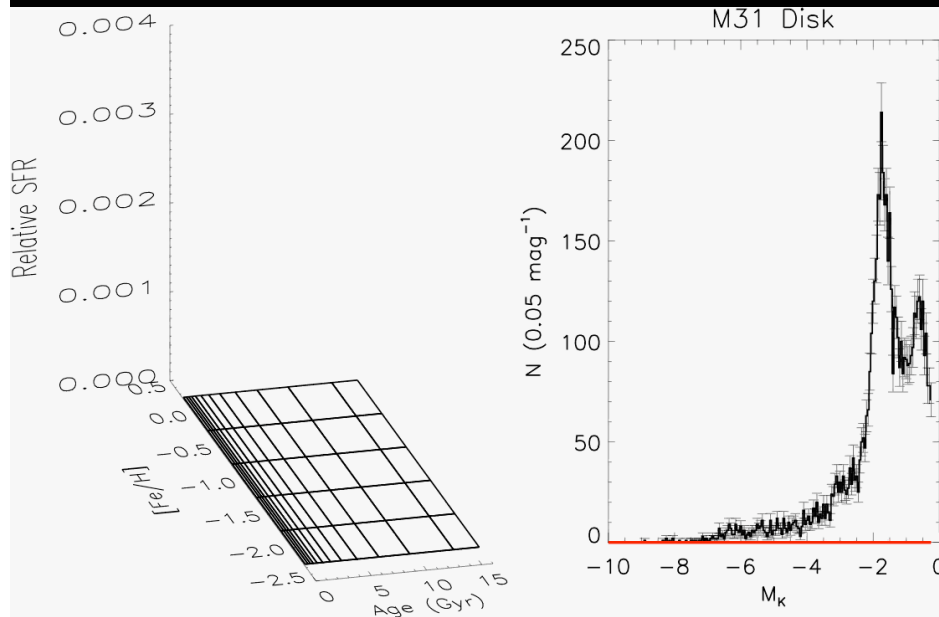
Deriving the population mix

- Build models from isochrones (Girardi et al. 2002):

Age = 1, 3, 5, 10 Gyr; $Z=0.0001, 0.0004, 0.001, 0.008, 0.019, 0.03$; Salpeter IMF for bulge and inner disk; finer age grid for Disk 2 field

- Apply photometric errors and incompleteness to models

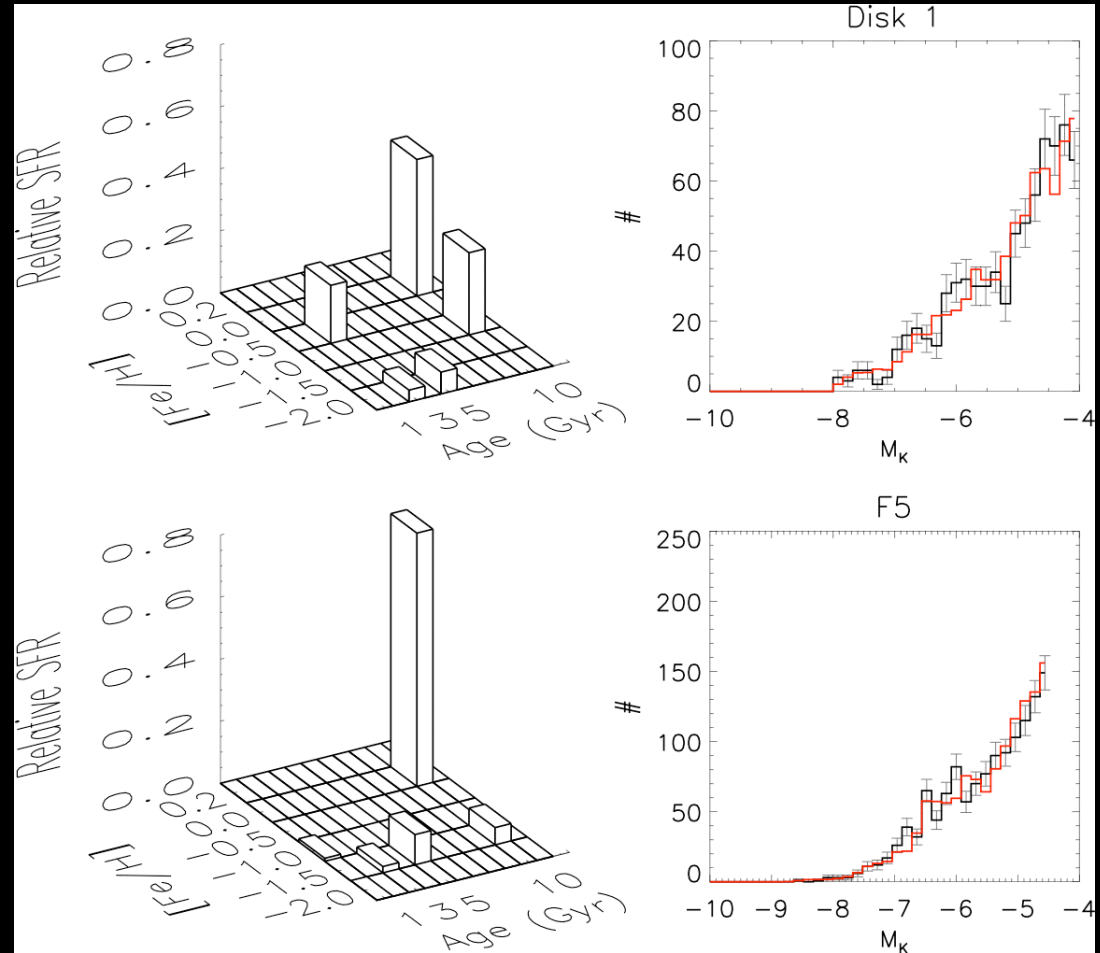
- Fit model mix to LFs using maximum likelihood analysis (Dolphin 1997, Olsen 1999, Dolphin 2002); assume $E(H-K)$ from IRAS/ISO; solve age and Z ; $(m-M)_0 = 24.45$



Results

Example: two
fields with Bulge/
Disk ~ 1

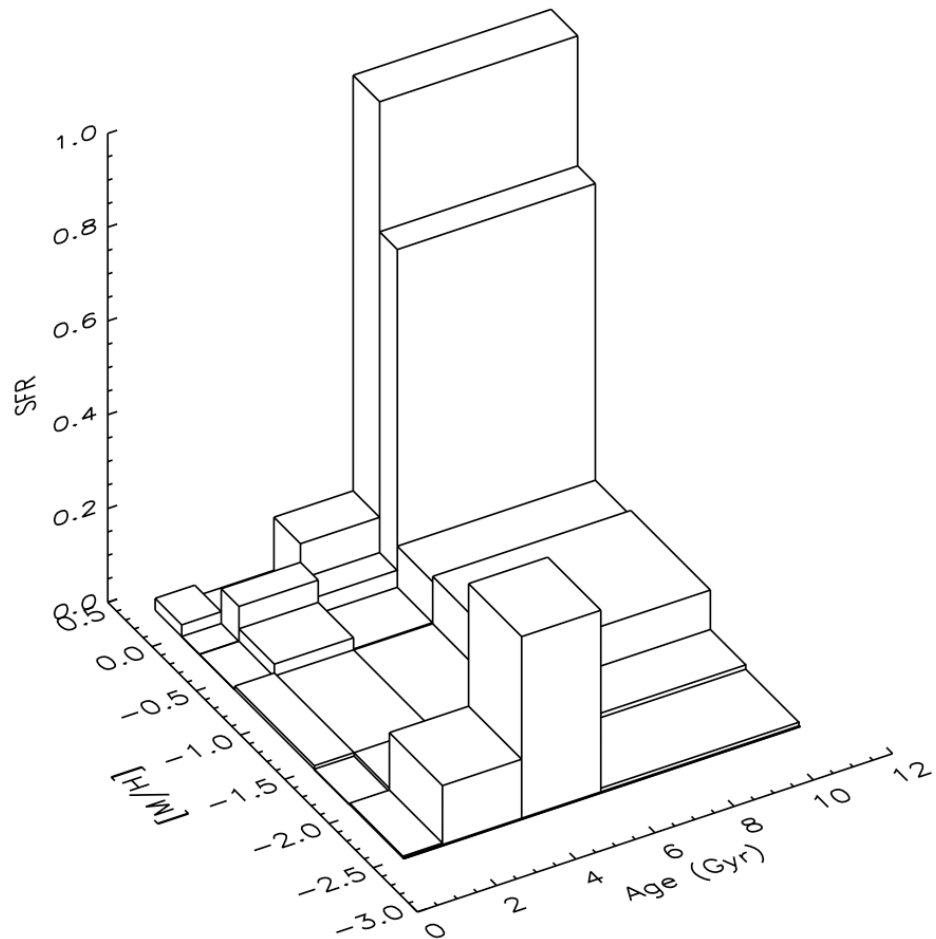
Fits are dominated
by the oldest
populations



Fit to LF: $P \sim 6 - 17\%$

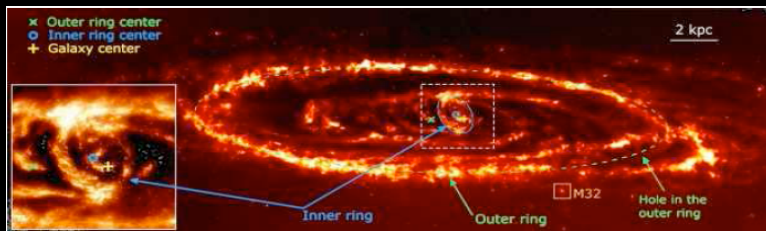
M31's Bulge and Inner Disk Population Box

- Old ages, nearly solar metallicities dominate
- Metal-poor intermediate-age populations are probably spurious
- Luminosity-weighted age, $[Fe/H] = 8$ Gyr, 0.0 (-0.5)
- Mass-weighted age, $[Fe/H] = 8.3$ Gyr, 0.0 (-0.4)

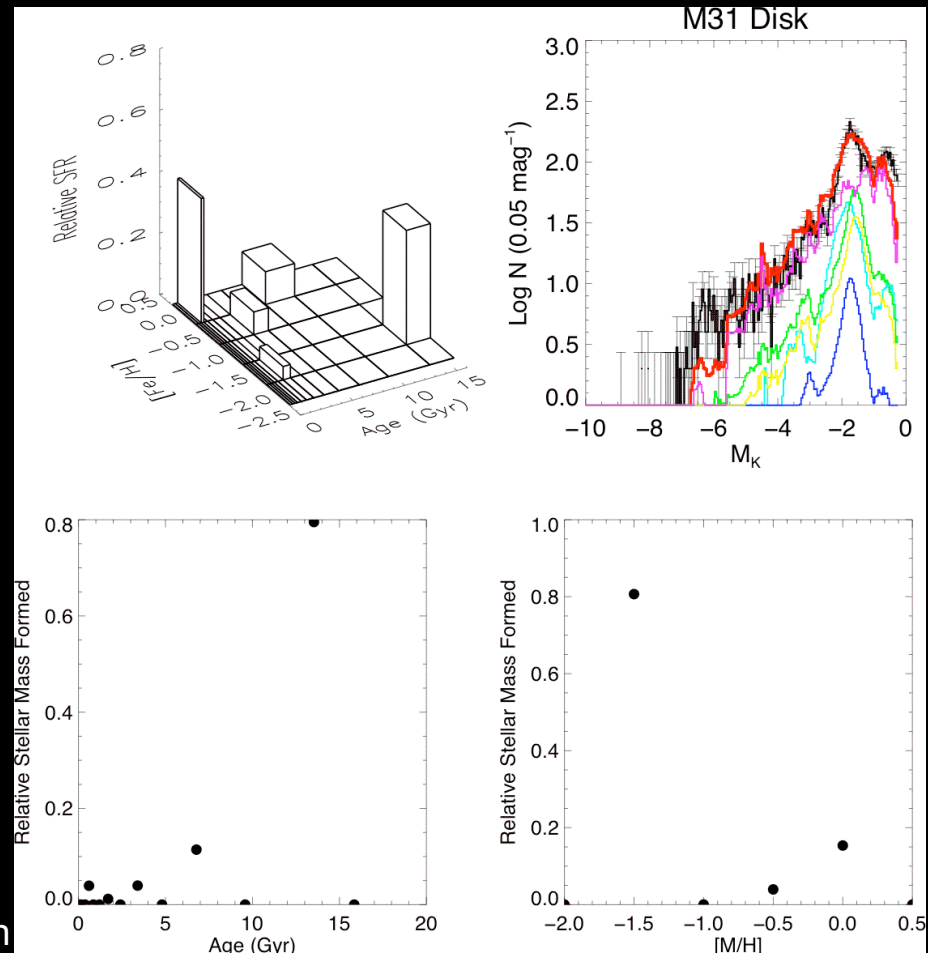


The Disk 2 Field

- 30% of stellar mass formed within last 250 Myr: prominent signature from the 10 kpc ring!
- 35% of the stellar mass appears ancient and metal-poor



Block et al. (2006): Suggest that a collision between M32 and M31 formed the rings ~210 Myr ago



Next: LGS Adaptive Optics

Increased sky
coverage of LGS
allows dense spatial
coverage of M31 disk
and comparison with
HST photometry

